

Human norovirus exhibits strain-specific sensitivity to host interferon pathways in human intestinal enteroids

Shih-Ching Lin^a, Lin Qu^{a,1}, Khalil Ettayebi^a, Sue E. Crawford^a, Sarah E. Blutt^a, Matthew J. Robertson^b, Xi-Lei Zeng^a, Victoria R. Tenge^a, B. Vijayalakshmi Ayyar^a, Umesh C. Karandikar^a, Xiaomin Yu^a, Cristian Coarfa^{b,c,d}, Robert L. Atmar^{a,e}, Sasirekha Ramani^a, and Mary K. Estes^{a,e,2}

^aDepartment of Molecular Virology and Microbiology, Baylor College of Medicine, Houston, TX 77030; ^bAdvanced Technology Cores, Baylor College of Medicine, Houston, TX 77030; ^cDuncan Cancer Center-Biostatistics, Baylor College of Medicine, Houston, TX 77030; ^dDepartment of Molecular and Cellular Biology, Baylor College of Medicine, Houston, TX 77030; and ^eDepartment of Medicine, Baylor College of Medicine, Houston, TX 77030

Contributed by Mary K. Estes, August 11, 2020 (sent for review June 3, 2020; reviewed by Carolyn B. Coyne and Miranda de Graaf)

Human noroviruses (HuNoVs) are the leading cause of viral gastroenteritis worldwide; yet currently, no vaccines or FDA-approved antiviral drugs are available to counter these pathogens. To understand HuNoV biology and the epithelial response to infection, we performed transcriptomic analyses, RT-qPCR, CRISPR-Cas9 modification of human intestinal enteroid (HIE) cultures, and functional studies with two virus strains (a pandemic GII.4 and a bile acid-dependent GII.3 strain). We identified a predominant type III interferon (IFN)-mediated innate response to HuNoV infection. Replication of both strains is sensitive to exogenous addition of IFNs, suggesting the potential of IFNs as therapeutics. To obtain insight into IFN pathway genes that play a role in the antiviral response to HuNoVs, we developed knockout (KO) HIE lines for IFN alpha and lambda receptors and the signaling molecules, *MAVS*, *STAT1*, and *STAT2*. An unexpected differential response of enhanced replication and virus spread was observed for GII.3, but not the globally dominant GII.4 HuNoV in *STAT1*-knockout HIEs compared to parental HIEs. These results indicate cellular IFN responses restrict GII.3 but not GII.4 replication. The strain-specific sensitivities of innate responses against HuNoV replication provide one explanation for why GII.4 infections are more widespread and highlight strain specificity as an important factor in HuNoV biology. Genetically modified HIEs for innate immune genes are useful tools for studying immune responses to viral or microbial pathogens.

human norovirus | interferon | enteroids/organoids | CRISPR-Cas9 | RNA-Seq

Human noroviruses (HuNoVs) are the leading cause of virus-induced gastroenteritis worldwide, causing significant morbidity and mortality in all age groups (1–4). HuNoVs are positive-sense, single-stranded RNA viruses in the *Caliciviridae* family with an RNA genome of ~7.7 kb that contains three open reading frames (ORFs): ORF1 encodes a nonstructural polyprotein, and ORF2 and ORF3 code for the major and minor capsid proteins, VP1 and VP2, respectively (5, 6). There are 10 norovirus genogroups, of which five (GI, GII, GIV, GVIII, and GIX) contain viruses that infect humans. Each genogroup is further divided into genotypes based on the sequence similarity of the capsid *VP1* gene and *RNA-dependent RNA polymerase (RdRp)* gene (7). The prototype Norwalk virus strain is designated GI.1, and the predominant genotype circulating worldwide is GII.4 HuNoV (8).

Although the first HuNoV outbreak was described in 1968, our knowledge of the mechanisms of HuNoV infection and their life cycle remains limited. This is largely due to the lack of a reproducible in vitro cultivation system for almost 50 y since the discovery of HuNoVs. Recently, several distinct ex vivo HuNoV cultivation systems including BJAB cells (9, 10), tissue stem cell-derived human intestinal enteroids (HIEs) (11), zebrafish (12), and human induced pluripotent stem cell-derived intestinal organoids (13, 14) have been reported. HuNoV replication in

HIEs recapitulates the tropism for intestinal enterocytes seen in patients (15), supports reproducible replication of multiple strains of HuNoV, confirms epidemiological differences in genetic susceptibility to infection, and has revealed strain-specific requirements for replication (11, 16–21). Specifically, the expression of genetically controlled histo-blood group antigens required for replication in HIEs mimics epidemiological patterns of virus infection in people (11, 21). Furthermore, studies using bile acid and ceramide, components of bile that are part of the intestinal milieu, have provided mechanistic insight into strain-specific requirements for HuNoV entry and replication in permissive cells (20). Thus, the HIE culture system allows new studies on HuNoV biology, virus–host interactions, antibody neutralization, and other antiviral interventions to be dissected.

One limitation of HuNoV replication in HIEs is the lack of indefinite serial passaging of virus, suggesting a role for uncharacterized host factors in limiting replication. Innate immune responses, including the synthesis and secretion of

Significance

Host innate immune responses are the first line of defense against viral infections, with the outcome of infection determined by the interplay between virus and host defense mechanisms. We report transcriptomic and functional analyses of epithelial cell responses to HuNoV infection in HIE cultures. HuNoV infection triggers predominantly a type III interferon (IFN) response and upregulation of long noncoding RNAs. Exogenously added IFNs restrict HuNoV replication in a strain-independent manner, but we unexpectedly found strain-dependent effects of endogenously activated cellular IFNs. Our findings suggest strain-specific sensitivities to IFN as a factor for global dominance of pandemic strains, provide a new arsenal of stable HIE knockout lines for several IFN pathways, and highlight strain differences as a consideration for development of effective therapies.

Author contributions: S.-C.L., R.L.A., and M.K.E. designed research; S.-C.L., L.Q., K.E., S.E.C., S.E.B., V.R.T., and B.V.A. performed research; S.-C.L., M.J.R., X.-L.Z., U.C.K., X.Y., and C.C. contributed new reagents/analytic tools; S.-C.L., M.J.R., C.C., S.R., and M.K.E. analyzed data; and S.-C.L., S.R., and M.K.E. wrote the paper.

Reviewers: C.B.C., University of Pittsburgh; and M.d.G., Erasmus University Medical Center.

Competing interest statement: M.K.E. is named as an inventor on patents related to cloning and cultivation of the Norwalk virus genome and is a consultant to and received research funding from Takeda Vaccines, Inc. R.L.A. has received research funding from Takeda Vaccines, Inc.

Published under the PNAS license.

¹Present address: Slaoui Center for Vaccines Research, GlaxoSmithKline Vaccines, Rockville, MD 20850.

²To whom correspondence may be addressed. Email: mestes@bcm.edu.

This article contains supporting information online at <https://www.pnas.org/lookup/suppl/doi:10.1073/pnas.2010834117/-DCSupplemental>.

First published September 9, 2020.

interferons (IFNs) and their downstream effectors, IFN-stimulated genes (ISGs), form a first line of defense against many viral infections (22–25). Studies of other human enteric viruses, including human rotavirus as well as murine norovirus, provide strong support for the role of IFN responses in controlling viral replication in mice and cultured cells; in many cases, there are strain-specific mechanisms by which these viruses antagonize host innate immune responses (26–29). To understand whether these host mechanisms restrict HuNoV replication, we have evaluated the epithelial response to infection in jejunal HIEs. Limited information is available regarding the role of innate epithelial responses in controlling HuNoV replication (30–33). We previously found that stool-derived HuNoV RNA transfected into mammalian cells, which bypasses virus entry but allows RNA replication, does not induce an IFN response. HuNoV RNA replication from transfected GI.1[P1] Norwalk virus stool RNA was sensitive to exogenously added type I (IFNA and IFNB) and type III IFN (IFNL) treatment but viral RNA replication was not enhanced by neutralization of type I/III IFNs or by blocking the IFN response (30). Antiviral effects of exogenously added IFNs have also been shown in several cell types expressing HuNoV replicons that, as with transfected stool RNA, do not recapitulate the full virus infection cycle (31, 34, 35). A recent study in HIEs indicates that HuNoV infection results in IFN-induced transcriptional responses through the JAK-STAT pathway (33). Our current studies demonstrate HuNoV infection of HIEs induces a robust innate response, which is predominately a type III IFN response dependent on active viral RNA replication. Exogenous IFN treatment abrogates replication of both GII.4 and GII.3 virus but unexpectedly, there are strain-specific differences in the response to intrinsic cellular IFN pathways wherein GII.3, but not GII.4, replication is reduced. Finally, GII.3 replication is significantly enhanced in *STAT1*-knockout HIEs mediated by increased permissiveness and virus spreading in these cultures.

Results

RNA Sequencing Reveals GII.4 HuNoV Infection Leads to Up-Regulation of ISGs. To evaluate intestinal epithelial responses to HuNoV, we infected monolayers of two susceptible, secretor-positive jejunal (J2 and J11) cultures with GII.4 virus. Mock- and gamma-irradiated GII.4 (gGII.4) inoculated cultures were used as controls. We performed RNA sequencing (RNA-Seq) to determine transcriptional responses to GII.4 at 6, 10, and 24 h postinoculation (hpi) in comparison to mock-inoculated cultures (3 hpi) or inoculation with gGII.4 HuNoV (6, 10, and 24 hpi). We have previously shown that the genetic background of the HIE cultures impacts analyses of transcriptional signatures to viral infections, with responses first clustering by HIE line (36). Based on these findings, the genetic background of the HIEs (J2 or J11) was treated as a blocking covariate in a linear model to determine the differential gene expression profiles. Principal component analysis (PCA) showed that gGII.4-inoculated and GII.4-infected samples had a similar early response to mock infections (Fig. 1A). At later times, the transcriptome profiles are more varied with clear separation seen at the 24 hpi between GII.4-infected and gGII.4-inoculated cultures (Fig. 1A and *SI Appendix, Fig. S1A*).

In concordance with the PCA results, no significant changes in transcription were seen in both GII.4-infected and gGII.4-inoculated samples at 6 hpi compared to media only at 3 hpi (*SI Appendix, Fig. S1B*). However, a progression in gene activation occurred with time, with transcriptional responses detectable by 10 hpi (Fig. 1B and *SI Appendix, Fig. S1B*). By 24 hpi, 529 genes were significantly up-regulated in GII.4-infected HIEs when compared to the media controls (Fig. 1B, false discovery rate [FDR] ≤ 0.05 and a fold change [FC] of at least 2) and 266 genes were up-regulated when compared to gGII.4 at 24 hpi (*SI Appendix, Table S1*), with ISGs accounting for the majority of up-

regulated genes. Since some changes in gene expression were also seen in gGII.4-inoculated cultures compared to media controls (Fig. 1B and *SI Appendix, Fig. S1B*) and we were interested in the kinetics of infection, we next determined the genes that are differentially expressed between GII.4-infected and gGII.4-inoculated samples and differentially changed with time (6 to 10 hpi and 10 to 24 hpi). There were no differentially detected genes between 6 and 10 hpi (Fig. 1C). Between 10 hpi and 24 hpi, 134 genes were up-regulated (FDR ≤ 0.05 and a FC of at least 2) in response to GII.4 compared to gGII.4 (Fig. 1C and D).

Next, we used gene set enrichment analysis (GSEA) to determine the pathways involved in the response to GII.4 infection for different time intervals (37). Controlling for the effect of potential immune modulators in stool using gGII.4, our GSEA analysis revealed that the top pathways up-regulated by GII.4 with time were IFN signaling and antiviral responses linked to ISGs (Fig. 1E and *SI Appendix, Table S1*), with a clear time-dependent increase in IFN signaling. These findings were also substantiated when gene expression was examined pairwise at each time point with reference to the media control infection (*SI Appendix, Fig. S1*). In contrast to the increases in IFN signaling, a time-dependent reduction in ribosomal RNA (rRNA) processing and translation was seen following GII.4 infection when compared to gGII.4 inoculation (Fig. 1E and *SI Appendix, Table S2*).

In concordance with the GSEA results, we observed a robust, statistically significant increase in expression of ISGs such as *IFI44L*, *MX1*, *IFIT1*, *IFIT3*, *IFITM1* and *STAT1* in GII.4-infected HIEs at 24 hpi, as well as other antiviral genes including *ADAR*, *EIF2AK2* (*PKR*) and *OASL* (Fig. 1F and *SI Appendix, Table S1*). Significant increases in the expression of type III IFN transcripts as well as *IFNB* but not *IFNA* were seen in both HIE lines compared to mock-infected cultures; this increase was not noted in gGII.4-inoculated HIEs. Although gGII.4 also induced some low-level ISG responses, these responses did not increase with time and are likely due to immune modulators present in the stool filtrate (*SI Appendix, Fig. S1*). To further evaluate indicators for activated IFN responses, we determined the effect of HuNoV infection on host long noncoding RNA (lncRNA) responses. lncRNAs are transcripts exceeding 200 nucleotides that are not translated into protein but are involved in gene regulation (38). A total of 192 lncRNAs were up-regulated following GII.4 infection at 24 hpi compared to mock-infected cultures and 48 lncRNAs were up-regulated when GII.4-infected samples were compared to gGII.4-inoculated samples at 24 hpi (*SI Appendix, Fig. S2A and Table S3*). Nine lncRNAs were differentially expressed between GII.4-infected and gGII.4-inoculated samples and differentially changed with time (10 to 24 hpi). While seven among the nine lncRNAs are nonannotated (*SI Appendix, Fig. S2B and C*), two lncRNAs (NRIR and BISPR) are both associated with IFN response (39, 40). In summary, the transcriptome data show that GII.4 HuNoV induces a robust ISG response and alters IFN-associated host lncRNAs. The up-regulation of ISGs and increase in IFN signaling observed from GSEA support a role for IFN in the response to viral infection.

GII.4 HuNoV Induces a Type III IFN Pathway in Jejunal HIEs. We hypothesized the contribution in antiviral pathways through ISGs might be primarily from the IFNL response, rather than IFNA or type II IFN (IFNG), because HIEs induce type III IFN in response to several viral infections (36, 41–46). Indeed, while increases in the expression of *IFNB* were seen along with type III IFNs in the gene expression (Fig. 1F), differential analysis showed very low expression of type I IFNs in HIEs. To validate the RNA-Seq results, we quantitated type I and type III IFN transcripts during HuNoV infection in J2 HIEs, which showed a more robust transcriptional response compared to J11 HIEs.

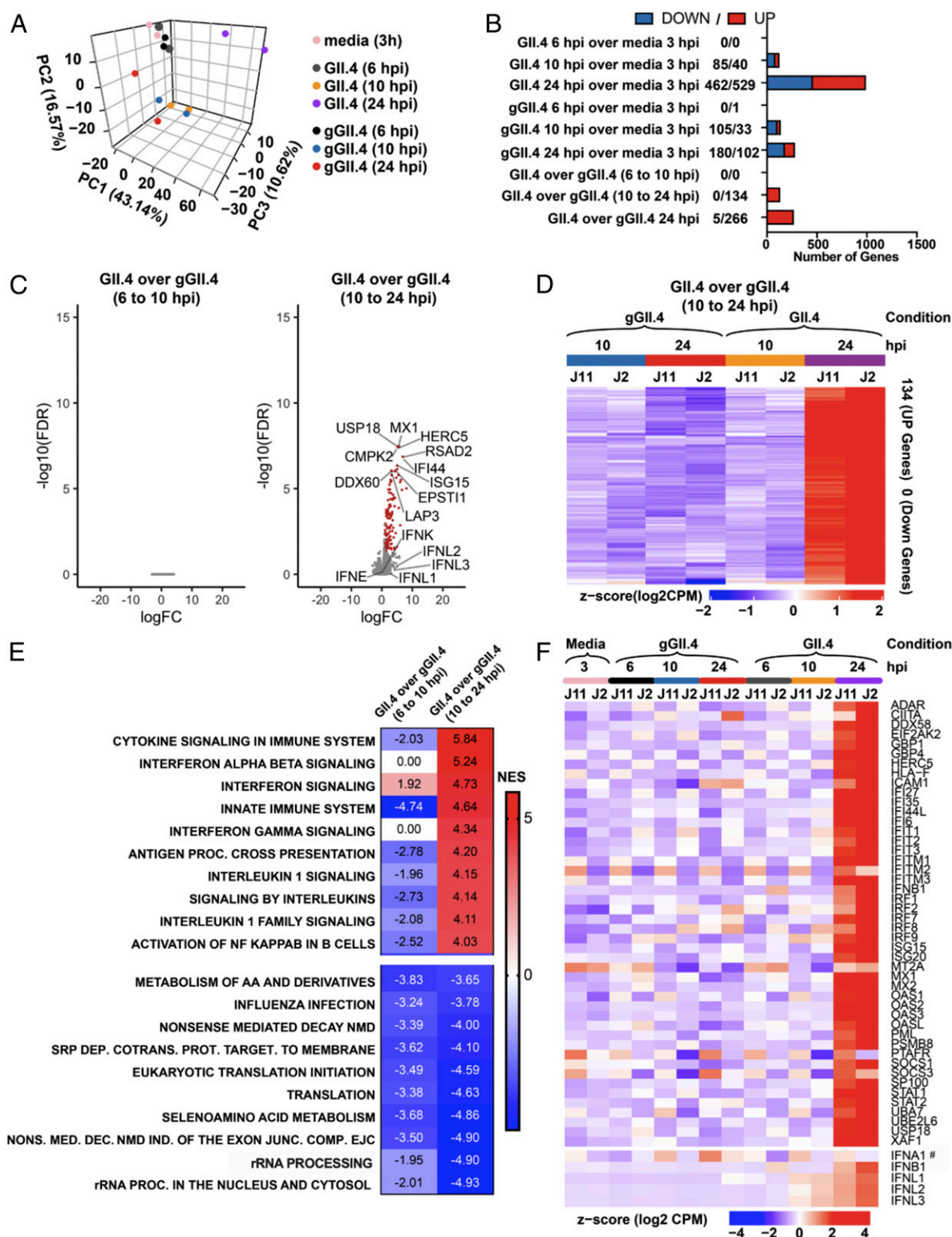


Fig. 1. GII.4 HuNoV induces robust IFN-stimulated gene responses in jejunal HIEs. Monolayer (J2 and J11) HIEs were inoculated with media, gamma-irradiated GII.4 (gGII.4) or infectious GII.4 (TCH12-580) stool filtrate containing 1.8×10^8 genome equivalents (GEs) of HuNoV for RNA-Seq analysis. (A) PCA was performed on the resulting normalized log₂ counts per million (cpm) expression matrix after correcting for the HIE genetic background. (B) The number of differentially up- and down-regulated genes (linear fold change of at least 2 and a FDR ≤ 0.05) is summarized in the bar chart. (C and D) Volcano plots and a heatmap of the differential gene analysis illustrate the progression of response with time. Genes were considered differentially expressed if they had a linear fold change of 2 and a FDR ≤ 0.05 , and are indicated using a red color in the volcano plot. (E) The up-regulated (top 10) and down-regulated (bottom 10) significant (FDR ≤ 0.25) Reactome pathways are ranked by the normalized enrichment score (NES) based on the changes in gene expression in GII.4-infected compared to gGII.4-inoculated cultures between 6 hpi and 10 hpi, and between 10 hpi and 24 hpi. (F) The statistically significant genes (fold change of at least 2 and a FDR ≤ 0.05 for any time point for the GII.4-infected or gGII.4-inoculated cultures compared to media controls) for selected IFNs and ISGs are visualized as heatmaps. # indicates that the change in *IFNA1* was not significantly different.

Cultures inoculated with GII.4 virus treated with a neutralizing antiserum served as a negative control, and the TLR3 agonist poly(I:C) was a positive control to induce IFN pathways. We chose a TLR3 agonist because HIEs express only a subset of TLRs, and TLR3 is the only receptor up-regulated by HuNoV infection in both J2 and J11 HIEs (*SI Appendix, Fig. S2D*). GII.4 replication was detected starting at 12 hpi (Fig. 2A). As expected, no viral RNA was detected in the mock-inoculated or poly(I:C)-treated wells, and no viral replication occurred when the GII.4 inoculum was neutralized by the HuNoV antiserum (Fig. 2A). Type I IFN transcripts (*IFNB1*) were induced to low levels following poly(I:C) treatment but not induced after HuNoV inoculation (Fig. 2B). In contrast, the type III IFN transcripts (*IFNL1*) were highly induced by poly(I:C) treatment and GII.4 infection as early as at 1 and 12 hpi, respectively (Fig. 2C). The induction of type III IFN transcripts at 12 hpi was concurrent with HuNoV replication (Fig. 2A). *IFNL1* induction was abrogated when the virus was neutralized by the antiserum, indicating the IFN responses were induced by HuNoV replication and not by other components of stool filtrate. In concordance with the RNA-Seq results, induction of ISG (*IFI44L*) was seen in GII.4-infected HIEs at 24 hpi but not when the virus infectivity was neutralized (Fig. 2D). These results were confirmed in two independent infected duodenal HIE lines. We next performed a Luminex assay to detect secreted IFN proteins from infected J2 and J11 HIEs at 96 hpi (Fig. 2E and F). Moderate *IFNL1* and high concentrations of *IFNL2/3* were produced from HIEs

infected with GII.4 or treated with poly(I:C), whereas the gamma-irradiated viruses only induced modest or low levels of IFNs in each HIE line. The *IFNB1* proteins were barely detectable in all groups. Responses varied in HIE lines with J2 HIEs being more responsive. In summary, our RT-qPCR and Luminex assay studies validated the RNA-Seq data and confirmed that HIEs respond to HuNoV replication and poly(I:C) treatment by inducing a predominant type III IFN response.

Exogenous IFN or Poly(I:C) Treatment Reduces GII.4 HuNoV Replication in HIEs. Knowing that HIEs elicit an IFN response against HuNoV infection, we next tested whether exogenously added IFNs or IFNs activated by poly(I:C) attenuate GII.4 HuNoV replication. Pretreatment with type I (*IFNA1* and *IFNB1*) or type III IFNs (*IFNL1*, *IFNL2*, and *IFNL3*) significantly attenuated GII.4 HuNoV replication compared with untreated control (Fig. 3A). Pretreatment with type III IFNs showed a greater effect on GII.4 replication compared to treatment at 1 hpi (*SI Appendix, Fig. S3A*). Pretreatment of HIEs with poly(I:C) at 24, 12, or 6 h before infection marginally attenuated GII.4 HuNoV replication compared with the untreated control at 24 hpi (Fig. 3B). By contrast, poly(I:C) treatment after inoculation had a reduced effect compared with pretreatment groups (Fig. 3B). ISG *IFI44L* expression at 1 hpi (Fig. 3C and D) was inversely proportional to GII.4 HuNoV replication, suggesting that the exogenously activated type I or type III IFN pathways were able to elicit antiviral responses to attenuate GII.4 HuNoV replication. This basal elevation of the

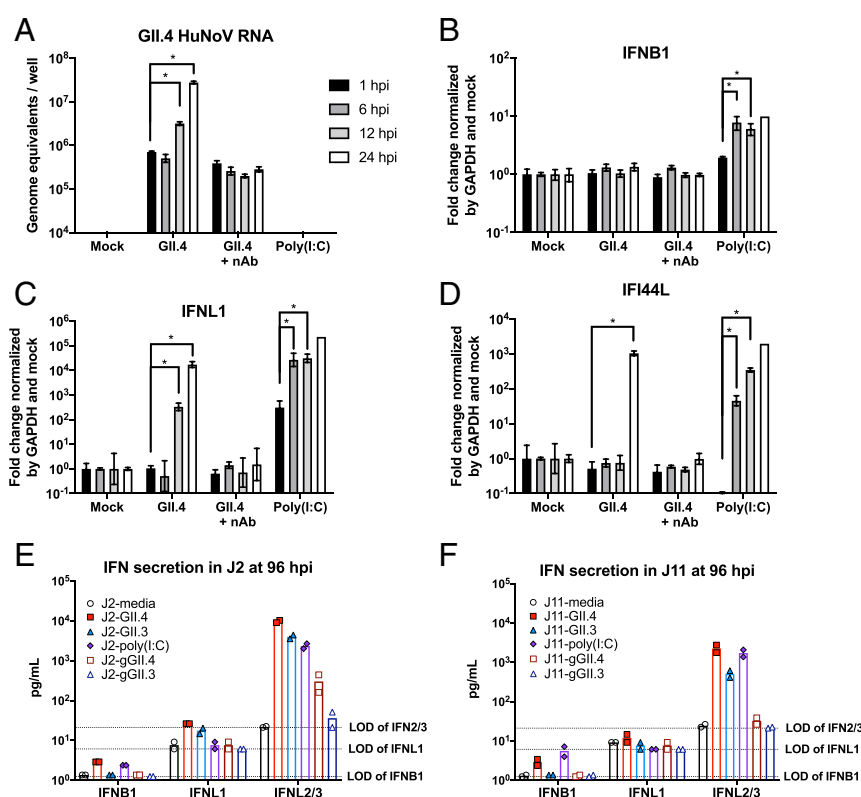


Fig. 2. GII.4 HuNoV induces a type III IFN pathway in jejunal HIEs. HIE (J2) monolayers were inoculated with media (mock), GII.4 (TCH12-580) HuNoV (9×10^7 GE/well), virus mixed with neutralizing antiserum (GII.4 + nAb) or treated with 100 μ g/mL of poly(I:C) in the presence of 500 μ M glycochenodeoxycholic acid (GCDCA). Poly(I:C) treatment of HIEs for the same time points without GII.4 inoculation served as the positive control. RNA extracted from the cells and medium was used to quantify (A) GII.4 HuNoV GE, (B) *IFNB1* transcripts, (C) *IFNL1* transcripts, and (D) ISG *IFI44L* transcripts. Each data bar represents the mean of three wells of inoculated HIEs, except for the mean of two wells of poly(I:C)-treated HIEs at 24 hpi. Error bars denote SD. * indicates $P < 0.05$. Each experiment was performed at least two times. For the Luminex assay, J2 and J11 HIEs were inoculated with media, GII.4 (TCH12-580, 9×10^7 GE/well), GII.3 (TCH04-577, 1.7×10^7 GE/well), 25 μ g/mL of poly(I:C), gamma-irradiated GII.4, or GII.3 HuNoV in the presence of 500 μ M GCDCA for 96 hpi. The concentration of *IFNB1*, *IFNL2*, and *IFNL2/3* proteins (pg/mL) (E) J2 and (F) J11 HIEs are shown. Dashed lines indicate the limit of detection (LOD) for each IFN. Supernatants from two wells for each condition and each HIE line were tested.

ISGs at 1 hpi by IFN pretreatment (Fig. 3 C and D) suggests the ISGs might impede HuNoV infection during the entry step. Overall, these data demonstrate GII.4 HuNoV replication is reduced by type I or type III IFN pathways exogenously activated prior to infection.

Inhibition of IFNs by an IFN Decoy Receptor Fails to Increase HuNoV Replication. Since exogenously added IFNs reduce HuNoV replication, we tested whether attenuation of the IFN pathways could enhance HuNoV replication. We used Y136, a decoy receptor for type I and type III IFNs that is produced by the Yabai-like disease virus (47) to attenuate IFN pathways in HIEs. Replication of GII.4 HuNoV was not enhanced by Y136 treatment in J2 HIEs (Fig. 3E) even though the Y136 treatment abrogated the induction of ISG *IFI44L* (Fig. 3F). The attenuation of *IFI44L* indicates that IFN proteins are induced following GII.4 replication and are secreted from infected HIEs; however, although Y136 was able to attenuate IFN downstream responses via chelating secreted IFNs, GII.4 replication was not enhanced by chemically inhibiting the endogenous IFN responses in HIEs.

Establishment of Knockout HIEs by Sequencing and Western Blotting. To further investigate whether endogenous type I or type III IFN pathways play a role in GII.4 HuNoV infection, we produced and evaluated whether the knockout (KO) of *IFNAR1* (the type I IFN receptor subunit), *IFNLRL1* (the type III IFN receptor subunit), *STAT1* (the master regulator of all three IFN pathways), or *MAVS* (the master regulator downstream of the TLR signaling pathways) alters the kinetics of GII.4 HuNoV replication in

HIEs. First, we transduced J2 HIEs with lentiviral vectors carrying *Streptococcus pyogenes*-derived Cas9 (Sp-Cas9) and the small guide RNA (sgRNA) targeting the *IFNAR1*, *IFNLRL1*, *STAT1*, or *MAVS* gene to generate the corresponding KO HIEs. Transduced HIEs were plated and expanded into single cell clones, and verified individually by genome sequencing, IFN treatment, and Western blotting. The *IFNAR1*-KO HIE contains a 6-bp deletion followed by a 1-bp insertion, indicating a 5-bp frameshift mutation in both alleles of the *IFNAR1* gene (SI Appendix, Fig. S4A). The *IFNLRL1*-KO HIE contains a 49-bp deletion as a frameshift mutation in both alleles of *IFNLRL1* gene (SI Appendix, Fig. S4C). Functional assessment of the KO lines showed that compared to the wild-type (WT) HIEs, treatment with the corresponding IFNs failed to induce ISGs in either *IFNAR1*-KO or *IFNLRL1*-KO HIEs (SI Appendix, Fig. S4B and D). Immunoblot and Western blot analyses showed that the *STAT1*-KO HIE does not express STAT1 protein (~91-kDa band indicated with an asterisk and the splice variant of 84 kDa as a lower band) (SI Appendix, Fig. S4E) while the *MAVS*-KO HIE does not express MAVS protein (~75-kDa band indicated with an asterisk) (SI Appendix, Fig. S4G). The basal level of *IFI44L* expression is lower in *STAT1*-KO HIEs compared with WT, and this ISG is not induced in mock-inoculated cells over 96 h (SI Appendix, Fig. S4F). Transfection of a *STAT2* sgRNA-expressing plasmid into the *STAT1*-KO HIEs was used to produce a *STAT1/STAT2*-double-KO (DKO) HIE line, also verified by genome sequencing and Western blot analysis for STAT1 and STAT2 (SI Appendix, Fig. S4H). These CRISPR-Cas9-generated IFN pathway-deficient HIEs designated *IFNAR1*-KO, *IFNLRL1*-KO,

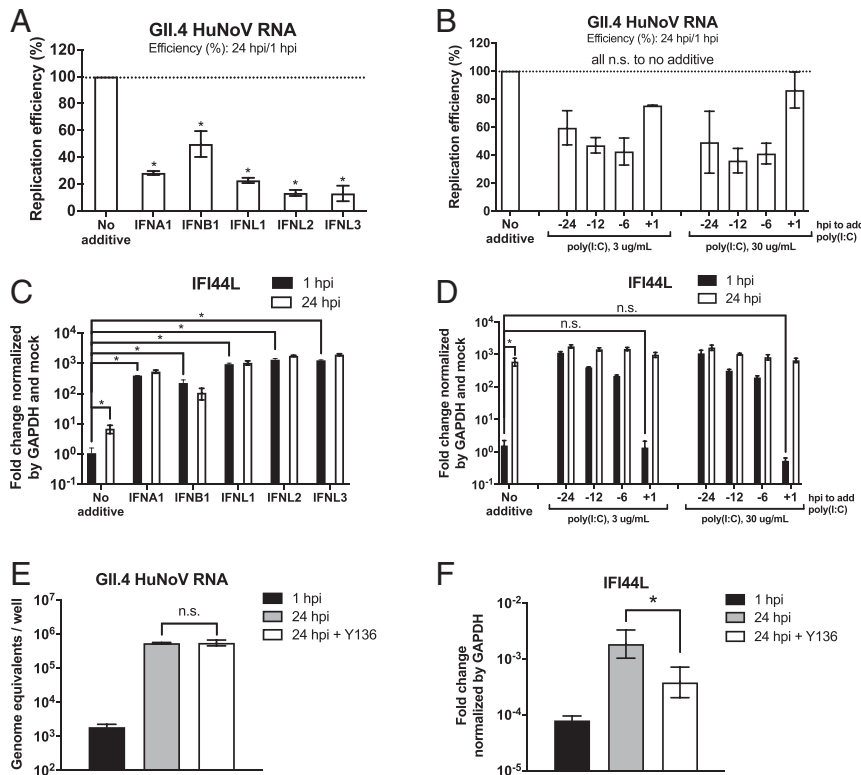


Fig. 3. GII.4 HuNoV replication is sensitive to exogenously activated IFN responses. HIE (J2) monolayers were preincubated with media only (no additive), 1,000 U/mL IFNA1 or IFNB1, or 100 ng/mL IFNL1, IFNL2, or IFNL3 for 24 h, or with 3 μ g/mL or 30 μ g/mL poly(I:C) at the indicated time points before inoculation with (A–D) 9×10^4 GE or (E and F) 1.8×10^5 GE of GII.4 (TCH12-580) stool filtrate (E and F) in the presence of 500 μ M GCDCA. Cells were cultured 24 h at 37 $^{\circ}$ C in the presence of GCDCA without (mock) or with the corresponding IFN (A and C) or with 25 μ g/mL of recombinant Y136 (E and F). Transcripts for HuNoV GEs (A, B, and E) or the ISG *IFI44L* (C, D, and F) were quantified by RT-qPCR. For A and B, each data bar represents the replication efficiency of treated wells relative to untreated wells at 24 hpi. Data were calculated by the mean of three wells of inoculated HIEs. Error bars denote SD. * indicates $P < 0.05$ and n.s. indicates $P \geq 0.05$. Each experiment was performed at least two times.

STAT1-KO, *MAVS-KO*, and *STAT1/STAT2-DKO* HIEs in a J2 WT background were then used to test for altered susceptibility to HuNoV infection and replication.

GII.4 HuNoV Replication Is Not Increased in IFN Pathway-Deficient HIEs with Attenuated ISG Induction. To assess the role of endogenous IFN pathways on GII.4 replication, we inoculated the WT and KO HIE lines with GII.4 and measured the kinetics of viral RNA replication at different times after infection by RT-qPCR. Infections were carried out at low multiplicity of infection (MOI) for these studies to allow for the evaluation of viral spreading over time. The replication kinetics of GII.4 HuNoV in all five KO HIEs were not enhanced compared with the WT HIEs (Fig. 4 A, C, and E). Significant induction of ISGs (as measured by *IFI44L* expression) in WT HIEs (Fig. 4 B, D, and F), was not altered by the loss of *IFNAR1* but was decreased by the loss of *IFNLR1* upon GII.4 infection (Fig. 4B), indicating HuNoV replication induces ISGs via type III IFN pathways. Further, the induction of ISGs was strongly attenuated in *STAT1-KO* and *STAT1/2-DKO* HIEs (Fig. 4 D and F, respectively) but only partially reduced in *MAVS-KO* HIEs upon GII.4 infection (Fig. 4D). These data indicate the induction of ISG *IFI44L* following GII.4 replication is *STAT* dependent, and partially *MAVS* dependent in HIEs.

Next, we tested the effect of exogenous IFN treatment on GII.4 replication in the KO HIEs. Pretreatment of IFNA1 or IFNL1 significantly reduced GII.4 replication in WT and *MAVS-KO* HIEs, but not in *STAT1-KO* HIEs (SI Appendix, Fig. S5A). The induction of ISG *IFI44L* by IFNs was significantly lower in *STAT1-KO* HIEs than in the WT HIEs (SI Appendix, Fig. S5B),

indicating HuNoV is sensitive to the JAK/STAT pathway induced by exogenous IFNs. We then evaluated whether the treatment of Y136 in *IFNAR1*, *IFNLR1*, *STAT1*, or *MAVS-KO* HIEs (SI Appendix, Fig. S6) compared to untreated groups would enhance GII.4 replication. In all KO lines tested, treatment with Y136 failed to enhance GII.4 replication (SI Appendix, Fig. S6 A and C) even though the ISG *IFI44L* expression was attenuated after treatment (SI Appendix, Fig. S6 B and D). Pretreatment with Y136 for 24 h before and after inoculation in *STAT1-KO* and *MAVS-KO* HIEs also failed to further enhance GII.4 replication (SI Appendix, Fig. S6E) although there was no induction of *IFI44L* (SI Appendix, Fig. S6F).

In summary, although the five IFN pathway-deficient HIE lines show attenuated ISG induction upon GII.4 infection, viral RNA replication kinetics are not altered in these KO lines, suggesting GII.4 replication is not sensitive to endogenous IFN responses during replication in jejunal HIEs.

GII.3 HuNoV Replication Is Increased in IFN Pathway-Deficient HIEs.

Unlike GII.4, GII.3 HuNoV requires bile acids to infect HIEs, indicating that different strains of HuNoVs have different entry requirements and may show varied responses to host cellular pathways. Therefore, we assessed the effects of IFN pathways on GII.3 (TCH04-577) replication. Similar to GII.4 HuNoVs, GII.3 also induces strong type III IFN secretion detected by the Luminex assay (Fig. 2 E and F). Pretreatment of WT HIEs with IFNA1, IFNB1, IFNL1, and IFNL3 reduced GII.3 replication (Fig. 5A). The basal expression of ISG *IFI44L* is higher at 1 hpi compared to untreated HIEs (Fig. 5B) and corresponds to the reduced replication in these treated cultures. Replication of

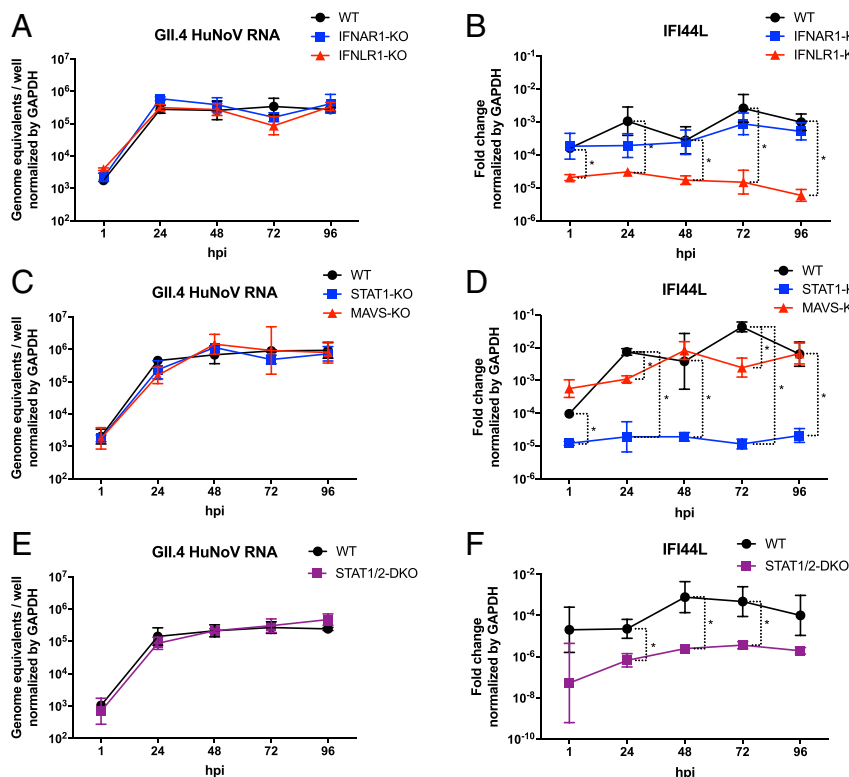


Fig. 4. GII.4 HuNoV replication is not increased in IFN pathway-deficient HIEs with attenuated ISG induction. WT, *IFNAR1-KO*, *IFNLR1-KO*, *STAT1-KO*, *MAVS-KO*, and *STAT1/STAT2-DKO* HIEs were inoculated with 9×10^4 GEs of GII.4 (TCH12-580) in the presence of 500 μ M GCDCA. Cells were cultured for either 24, 48, 72, or 96 h at 37 °C in the presence of GCDCA. RNA was extracted at different time points for RT-qPCR to quantify (A, C, and E) GII.4 HuNoV GEs or (B, D, and F) ISG *IFI44L* transcripts. Each data bar represents the mean of three wells of inoculated HIEs. Error bars denote SD. * indicates $P < 0.05$. Each experiment was performed at least two times.

GII.3 HuNoV also was not enhanced by Y136 treatment (Fig. 5C) although *IFI44L* expression was reduced (Fig. 5D). We next inoculated WT and KO HIE lines with GII.3 and measured viral replication kinetics to determine whether GII.3 replication is similarly insensitive to endogenous IFN pathways as seen for GII.4 HuNoV replication. In contrast to GII.4, GII.3 HuNoV replication was increased 10 to 100-fold in *STAT1-KO* and *IFNAR1-KO* HIEs, respectively, compared with replication in WT or other KO HIE lines (Fig. 6A and C), and the enhanced replication was accompanied by reduced ISG responses (Fig. 6B and D), indicating that the endogenous IFN pathway is a restricting factor that blunts GII.3 HuNoV replication in HIEs. Although ISG expression was reduced, GII.3 replication was not enhanced in *STAT1/2-DKO* HIEs (Fig. 6E and F).

We next performed fluorescent focus assays (FFAs) to evaluate whether the increased levels of GII.3 RNA replication were associated with increased viral spreading in the HIE cultures. Significantly higher numbers of GII.3-positive cells were detected in *STAT1-KO* monolayers compared with WT monolayers (Fig. 7A and B) and clusters of GII.3-positive cells increased over time (Fig. 7C and SI Appendix, Fig. S7B), with cells being lost from the monolayer by 96 hpi compared with infections in WT HIEs (SI Appendix, Fig. S7B). To evaluate whether *STAT1-KO* HIEs are more susceptible to GII.3 infection, we next determined the tissue culture infectious dose (TCID₅₀) for GII.3 infection in WT and *STAT1-KO* HIEs by the Reed–Muench method (48). The TCID₅₀ for GII.3 infection of WT J2 HIEs was 7.94×10^4 GEs/well, and the TCID₅₀ for *STAT1-KO* HIEs was 3.42×10^3 GEs/well, suggesting that the latter genetically modified HIE line is more permissive for GII.3 infection (Fig. 7D). These results indicate that differences in GII.3 replication seen in the time-course experiments could be due to enhanced susceptibility of KO cells during the first round of infection as well as increased virus spreading during the subsequent rounds of infection in the *STAT1-KO* HIEs. In contrast, *STAT1-KO* HIEs were not more susceptible to GII.4 as determined by FFA (SI Appendix, Fig. S7A). In conclusion, GII.3 HuNoV replication is sensitive to host endogenous IFN pathways and knockout of *STAT1* in particular increases viral replication and spreading, a response that is distinct from the unresponsiveness of GII.4 replication even in cultures with abrogated host IFN responses.

Discussion

The host innate response is the first line of defense following infection, and the outcome of infection is governed largely by an interplay between the virus and host antiviral defenses. To efficiently combat HuNoV disease, it is necessary to understand the viral life cycle and whether viral replication is affected by host restrictions. Here, we show that HuNoV infection induces a robust innate response concomitant with viral RNA replication and ISGs are induced by a predominant type III IFN response. Functional and CRISPR knockout studies revealed the innate responses differentially affect replication of two distinct HuNoV strains relative to intrinsic cellular IFN signaling pathways, with increased replication and virus spreading occurring in *STAT1-KO* cultures infected with GII.3, but not GII.4, virus. Given the epidemiological differences in the prevalence of these strains, the lack of restriction of GII.4 HuNoV replication by the innate cellular response may explain why these strains predominate in the human population (8).

Before the discovery of the HIE-based HuNoV ex vivo culture system, innate immune responses to HuNoV RNA replication were examined by using human hepatoma (HG23) or gastric tumor (HGT) cell-based GI.1 replicon systems (31, 49, 50), and human embryonic kidney (293FT) cells transfected with authentic GI.1 HuNoV RNA from stools of infected persons or RNA expressed from a reverse genetics full-length GII.3 plasmid (30). The main limitation to these previous studies is that none represented a complete virus infection cycle; in particular, the viral entry step was missing, which itself can induce innate responses, and the sites of RNA replication may have been in cytoplasmic compartments different from those in an authentic viral infection.

Thus, our overall understanding of the host response to HuNoV infection remained limited, and the HIE replication system for HuNoVs offered the opportunity to examine the innate epithelial responses in multicellular, nontransformed, fully permissive human epithelial cultures. One study reported limited GII.4 virus replication in jejunal HIEs (1.55- to 17.23-fold increases of genome equivalents) and induction of host IFN responses, with a 3-fold increase of *IFNL* gene expression at 72 hpi (32). An innate response was detected based on ISG gene expression 48 hpi of ileal HIEs with live, but not heat-inactivated

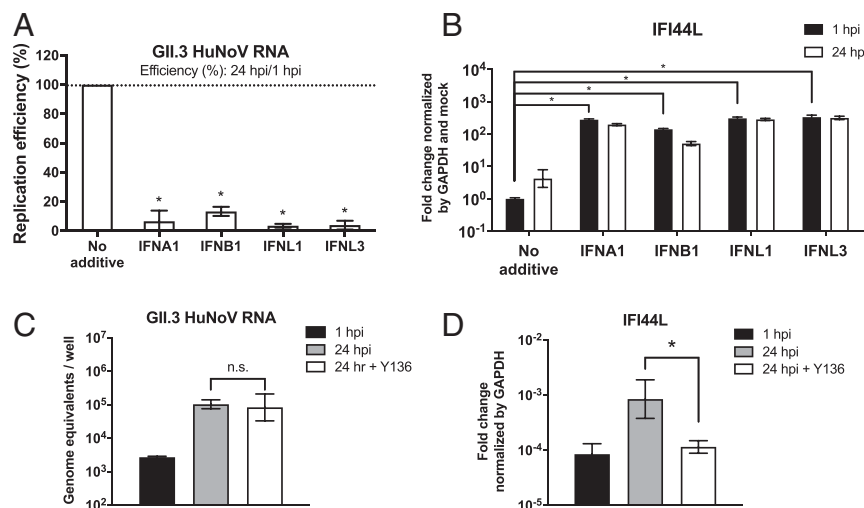


Fig. 5. Exogenous IFN reduces GII.3 HuNoV replication in HIEs. HIE (J2) monolayers were preincubated with media only (no additive), 1,000 U/mL IFNA1 or IFNB1, or 100 ng/mL IFNL1 or IFNL3 for 24 h, then inoculated with (A and B) 4.3×10^5 GEs or (C and D) 8.6×10^5 GEs of GII.3 (TCH04-577) stool filtrate in the presence of 500 μ M GCDCA. Cells were cultured 24 h at 37 °C in the presence of GCDCA without or with the corresponding IFN. RNA was extracted at different time points for RT-qPCR to quantify (A and C) GII.3 HuNoV GEs or (B and D) ISG *IFI44L* transcripts. Data were calculated by the mean of three wells of inoculated HIEs. Error bars denote SD. * indicates $P < 0.05$ and n.s. indicates $P \geq 0.05$. Each experiment was performed at least two times.

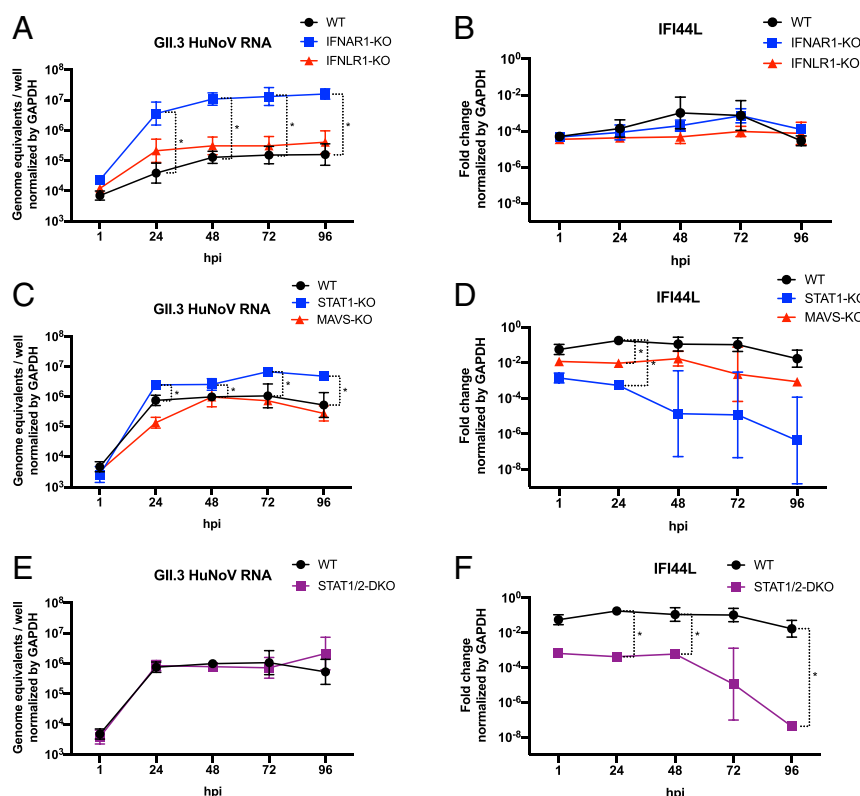


Fig. 6. GII.3 HuNoV replication is increased in IFN pathway-deficient HIEs. WT, *IFNAR1-KO*, *STAT1-KO*, *MAVS-KO*, and *STAT1/2-DKO* HIEs were inoculated with 4.3×10^5 GE of GII.3 (TCH04-577) in the presence of 500 μ M GCDCA. Cells were cultured for either 24, 48, 72, or 96 h at 37 °C in the presence of 500 μ M GCDCA. RNA was extracted at different time points for RT-qPCR to quantify (A, C, and E) GII.3 HuNoV GE for the replication kinetics or (B, D, and F) ISG *IFI44L* transcripts. Each data bar represents the mean of three wells of inoculated HIEs. Error bars denote SD. * indicates $P < 0.05$. Each experiment was performed at least three times.

GII.4 HuNoV (33). The strain of GII.4 or GII.3 was not reported in either study.

Our RNA-Seq data from infections of two jejunal HIE lines with different genetic backgrounds inoculated with live and gGII.4 Sydney virus report time-dependent innate responses with type III IFN pathways (*IFNL* genes) being up-regulated in conjunction with the onset of viral RNA replication followed by robust up-regulation of IFN signaling and ISG expression in both HIE lines. HuNoV RNA replication, which begins by 12 hpi and reaches 10^2 - to 10^3 -fold increases in viral genome equivalents at 24 hpi, is accompanied by a 10^2 - to 10^3 -fold up-regulation of type III IFN transcripts compared to 1 hpi, while type I IFN transcripts only marginally increase (less than 10-fold) even with HIE stimulation with the potent TLR3 agonist poly(I:C). These results indicate HIEs preferentially induce type III IFN pathways instead of type I IFN pathways after HuNoV infection, and the onset of IFN responses begins at 10 to 12 hpi concurrent with HuNoV RNA replication. The predominant type III IFN gene expression mirrors data from HIE infections with human rotavirus (36), enterovirus in fetal HIEs (46, 51), and astrovirus in duodenal HIEs, although astrovirus infection of duodenal HIEs also induced type I (*IFNB*) (45). Moreover, the replication-dependent induction of IFN indicates HIEs detect the replicating genome as pathogen-associated molecular pattern molecules to induce IFNs via TLR pathways, which correlates with the up-regulation of *TLR1* and *TLR3* expression after infection (SI Appendix, Fig. S2). Observations from our data are reduced transcription of genes involved in rRNA processing and translation following HuNoV infection and increases in a subset of lncRNAs. Only two (NRIR and BISPR) of the nine up-regulated lncRNAs are annotated and both are associated with IFN

responses (39, 40). NRIR is reported to share loci with host ISG *CMPK2*, and BISPR shares loci with host ISG *BST2*. *CMPK2* and *BST2* are up-regulated with HuNoV infection as well (SI Appendix, Table S1). The biological significance of these regulatory pathways remains to be elucidated.

Further dissection of the importance of these innate HIE responses to control HuNoV infection yielded unexpected differing results depending on whether exogenous IFN treatment of cultures or intrinsic cellular IFN signaling was evaluated as well as which virus strain was used in the infectivity studies. Exogenous IFN treatment of cultures reduced replication of both GII.4 and GII.3 HuNoV strains, similar to effects seen in the early replicon studies noted above and studies with rotavirus (36) and astrovirus infection in HIEs (45). Pretreatment of cultures with high doses of type I or type III IFN to HIEs before infection triggered ISG expression to a high level and resulted in interference with infection, attenuating replication of GII.4 (60 to 80%) and GII.3 (70 to 90%) HuNoVs. These significant decreases suggest that viral entry and replication were impaired when ISGs were activated by IFN treatment prior to infection. Interestingly, replication of GII.3 was more sensitive to the same doses of recombinant IFNs than GII.4, providing an indication of strain-specific differences in HuNoV responses to IFN signaling. Exogenous IFN treatment studies and inhibition of HuNoV replication suggest IFNs could be a viable therapeutic strategy to consider for HuNoV infection especially for chronically infected patients who can suffer with diarrhea for years (52). Type III IFNs may be the preferred treatment to assess further because of its reported reduced side effects compared to type I IFNs (53, 54). Additional preclinical evaluation of type III IFN treatment on the replication of more viral strains, including

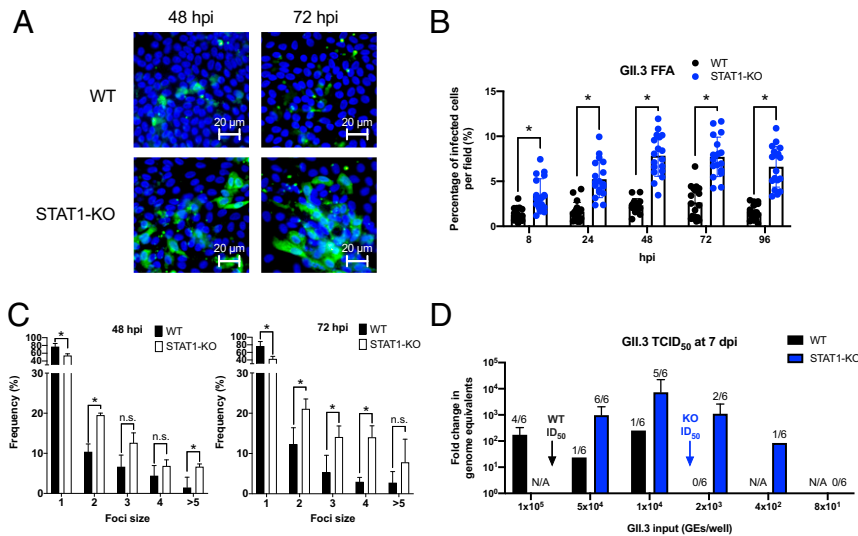


Fig. 7. *STAT1-KO* HIE cells are more susceptible to GII.3 infection. HIE monolayers were inoculated with 4.3×10^6 GEs of GII.3 (TCH04-577) (A–C), or the indicated GEs/well (D) in the presence 500 μ M GCDCA. Cells were cultured in the presence of GCDCA for indicated times for FFA (A–C) or (D) 7 d for TCID₅₀. (A) GII.3-positive cells (green) were detected after staining with guinea pig anti-HuNoV Ab with nuclei (blue) stained by DAPI. Infected cells in clusters identified viral spreading. (B) Numbers of infected cells were calculated in six independent images per condition and each experiment was performed in triplicate ($n = 18$ in total). (C) The frequency of foci of different sizes was determined from six independent images per condition at 48 and 72 hpi in triplicate experiments ($n = 18$ in total). (D) Fold changes of GII.3 RNA replication at 7 d compared to 1 hpi and the numbers of positive wells at each inoculum dose were used to determine the TCID₅₀ in WT and *STAT1-KO* cultures. * indicates $P < 0.05$ and n.s. indicates $P \geq 0.05$. Each experiment was performed at least two times.

those from chronically infected patients, and using a wider range of HIEs from different intestinal segments and donor backgrounds is needed.

Independent studies evaluating whether neutralization of secreted IFNs using an IFN decoy receptor (Y136) would enhance HuNoV replication indicated that HuNoV may be able to avoid host restriction based on IFN induction. Y136 successfully reduced ISG induction following GII.4 and GII.3 infection, indicating IFNs secreted into the medium were neutralized; yet, virus replication remained unchanged. These results are consistent with the less than twofold change of GII.4 replication (compared to the dimethyl sulfoxide [DMSO] vehicle control) seen in a recent study using the JAK inhibitor ruxolitinib that reduced ISG induction, but contrast with the approximate sixfold enhancement of GII.3 replication (33).

Genetic modification to knock out genes for IFN pathways with CRISPR-Cas9 provided the clearest validation of the impact of intrinsic cellular IFN signaling pathways on GII.4 replication. Cas9 genome editing has been used to knock out genes in HIEs, including *CFTR* (55), *STAT2* (56), and *FUT2* (21). We knocked out the type I and type III IFN receptors, *STAT1*, *STAT2*, and *MAVS* to deplete either or both the type I IFN and type III IFN pathways or mediators for several TLR pathways. Surprisingly, GII.4 replication remained unchanged in all KO HIEs with deficient IFN pathways and attenuated ISG induction. These results indicate GII.4 replication is not affected by the presence of cellular IFN responses in HIEs even though this virus is sensitive to exogenous treatment of cultures with IFN. A striking distinct phenotype was observed for GII.3 HuNoV, which replicated better in *STAT1-KO* and *IFNARI-KO* HIEs with ~10- to 100-fold increases, respectively, indicating replication of this virus is sensitive to endogenous IFN signaling triggered by the virus. Our genetic studies extend previous findings of ~6-fold enhancement of GII.3 replication in HIEs modified by expression of NPro protein from bovine diarrhea virus (BVDV) and V protein from parainfluenza virus type 5 (PIV5 V), two viral innate immune antagonists known to suppress the innate response. Modest increases in replication in cultures

expressing BVDV NPro or PIV5 V may be due to incomplete KO using the viral antagonists. GII.4 replication was not compared in the previous studies with BVDV NPro and PIV5 V to know whether a differential effect would have been seen compared with GII.3 replication (33).

An important question was whether the improved RNA replication of GII.3 in the *STAT1-KO* cells is caused by an increase in the numbers of infected cells or virus spreading or both. Significant HuNoV spreading has not been shown previously in any cell line. GII.3 infection of the *STAT1-KO* cultures showed infection of clusters of cells that increase in number and size with time. This demonstration of HuNoV spread in infected cultures is remarkable. The *STAT1-KO* line is also more susceptible to GII.3 infection as demonstrated by the lower TCID₅₀ required for infection, which could be due to less restriction of entry in neighboring cells when viruses are released from the first infected cells. This sharply contrasts the limited fluorescent foci and lack of spreading over time seen in WT or *STAT1-KO* infected with GII.4 virus. These results further indicate that GII.4 can avoid the endogenous IFN responses, although it is possible there may be other restricting factors, including IFN-independent antiviral pathways that still restrict GII.4 replication. Although down-regulation of IFN pathways play a role, the exact mechanistic basis for the increased susceptibility of GII.3 HuNoV remains to be defined. In addition, the increased susceptibility has not resulted in the ability to indefinitely passage GII.3 in *STAT1-KO* HIEs, suggesting other unrecognized factors play a role in limiting replication.

The differences of GII.3 replication in *IFNLR1-KO* compared to *IFNARI-KO* and *STAT1-KO* HIEs are remarkable. First, although the predominant response of HIEs is activation of type III IFN pathways against viral infection based on our RNA-Seq and RT-qPCR results, GII.3 RNA replication was enhanced in type I IFN pathway-deficient HIEs compared to replication in the type III pathway-deficient HIEs. This was unexpected but type I IFN pathways may still dominate in HuNoV restriction in enterocytes. In addition, the mucosal-specific type III IFN pathways may not be directly antiviral but may have alternative

effects on bystander epithelial and/or nonepithelial cells or they may mediate tissue repair or communicate with immune cells and microbiota in vivo. Signaling of type III IFN with immune cells, currently lacking in the epithelial-only HIE cultures, has been shown to be important for innate and adaptive immune responses in human cells, which is different from previous conclusions from studies in mice (57). Other roles of type III IFN have also been postulated from studies with human rotavirus infection in HIEs where the virus is not restricted by the predominant type III IFN response in HIEs, although this is partially due to mechanisms of rotavirus antagonism of the innate response (36, 58).

The roles of endogenous IFN pathways have been studied in many RNA viral infections including two other enteric viruses, rotavirus and murine norovirus (MNV). *STAT1*-dependent innate immunity is essential for control of acute MNV infection of mice (59), and virus replication is enhanced in *STAT1*-deficient immune cells in vitro (60). *IFNLR1* depletion enhances replication of the persistent MNV CR6 strain in mice with IFNLR treatment (61). Therefore, the enhanced replication of a HuNoV GII.3 strain in *STAT1*-KO HIEs is not surprising; however, the unchanged replication of the globally predominant HuNoV strain in these same KO cells was unexpected. Why GII.4 infection is not sensitive to the depletion of endogenous IFN pathways remains unknown. There are many mechanisms by which other viruses evade IFN-mediated antiviral responses (27) and understanding how GII.4 HuNoV overcomes IFN signaling, and what host factors restrict GII.4 HuNoV replication in *STAT1*-KO cells are important to dissect the pathogenesis of this clinically relevant virus strain and to develop interventions. Unexpectedly, infection of the *STAT1/2*-DKO HIEs did not enhance HuNoV replication. Additional characterization of this line is required to evaluate if addition of two sgRNAs to HIEs results in stress responses that impede culture growth or virus replication.

The discovery of differences in sensitivity to intrinsic IFN pathways of two HuNoV strains adds to a growing list of strain-specific distinct biological behaviors of HuNoVs. Differences in binding to histo-blood group antigens, glycans whose expression is genetically encoded by host fucosyltransferases, that are required as initial binding factors for infection was one of the first examples of strain-specific differences in HuNoV biology (11, 21, 62–64). More recently, strain-specific differences in requirement for bile or bile acids for infection of HIEs (20) and induction of host adaptive immune responses by GII.2 HuNoV (65) have been described. Recognition of strain-specific differences in sensitivities to innate responses provides insights into the spectrum and heterogeneity of HuNoV biology and may provide an explanation for why specific pathogenic strains may be more widespread than others. Finally, the KO HIE cultures will likely be important tools to characterize the properties of other HuNoV strains such as GII.17, which emerged quickly and remained widespread for several years. These cultures are also useful for studying noncultivable HuNoVs as well as other human viruses that replicate in the gastrointestinal tract, including sapovirus or even the pandemic SARS-CoV-2 (66), where the innate immune response is still considered to be the primary restricting factor for their replication.

Materials and Methods

Detailed methods and descriptions of viruses, cells, and infections; RNA extraction and RT-qPCR (67, 68); differential gene expression analysis (37, 69); Luminex assays; cytokines, agonists and antibodies; HIE transduction and single-cell cloning; and protein extraction, Western blotting, and immunofluorescent staining are provided in *SI Appendix, SI Materials and Methods*.

RNA-Seq Analysis. We performed RNA-Seq analysis on two differentiated jejunal HIE lines (J2 and J11), inoculated with mock, gamma-irradiated GII.4

or infectious GII.4 at high MOI infection (1.8×10^8 genome equivalents/well). Total cellular RNAs were extracted from 5-d differentiated, mock-inoculated monolayers at 3 hpi, and GII.4- or gII.4-inoculated monolayers at 6, 10, and 24 hpi using RNeasy Mini Kit (Qiagen). The RNA integrity was assessed on a 2100 Bioanalyzer (Agilent). A double-stranded cDNA library was created using 500 ng of total RNA (measured by picogreen), preparing the fragments for hybridization onto a flowcell. An ERCC RNA Spike-In Control Mix 1 was added to each sample according to the manufacturer's protocol. First, cytoplasmic and mitochondrial ribosomal RNA was removed from the total RNA samples using Illumina's Epidemiology-Specific RiboZero rRNA removal protocol. Then cDNA was generated using the fragmented and rRNA-depleted total RNA using random primers. During second-strand synthesis, deoxythymidine triphosphate (dTTP) was replaced with deoxyuridine triphosphate (dUTP) which quenches the second strand during amplification, thereby achieving strand specificity. Libraries were created from the cDNA by first blunt ending the fragments, attaching an adenosine to the 3' end, and finally ligating unique adapters to the ends for PCR amplification. Paired end sequencing (2×100 bp) was performed on an Illumina HiSeq 2500 for a depth of 30 million paired end reads (a total of 60 million reads) per RNA sample. The fastq files generated during sequencing were quality trimmed using Trim Galore (70, 71). Trimmed reads were then aligned to GRCh38 using Hisat2 and then a count matrix was generated from the aligned reads using featureCounts (72). The RNA-Seq data files and raw count matrix files were deposited in the Gene Expression Omnibus (GSE150918).

Cas9/sgRNA-Expressing Vector Cloning. The sgRNA sequences for several target innate genes including IFN receptors and pathway mediators are indicated in *SI Appendix, Table S4*. Each sgRNA sequence was cloned into the LentiCRISPR v2 plasmid (Addgene, 52961) or Hygro-LentiCRISPR v2 plasmid (purchased from the Cell-Based Assay Screening Service [C-BASS] core at BCM) by *BsmBI* digestion and ligation as previously described (73).

Lentiviruses which express Cas9 and sgRNA were packaged by cotransfecting pMD2.G (Research Resource Identifiers [RRID]: [Addgene_12259](#)), psPAX2 (RRID: [Addgene_12260](#)), and the designed LentiCRISPR v2 with sgRNA into HEK-293FT cells (ATCC, PTA-5077, RRID: [CVCL_6911](#)) using a polyethylenimine (PEI) transfection reagent (Sigma). The supernatant was harvested every 24 h until 72 h posttransfection and concentrated by polyethylene glycol (PEG)-6000 and sodium chloride precipitation, suspended in complete medium with growth factors [CMGF(+)], aliquoted, and then stored at -80°C . HIE KO lines were generated following transfection and single-cell selection as described in *SI Appendix, SI Materials and Methods*.

Quantification and Statistical Analysis. For RT-qPCR, fold changes in mRNA expression for host genes were determined using the delta-delta-Ct method relative to the values in control samples as indicated in the figure legends, after normalization to the housekeeping gene GAPDH (74). Results are presented as means \pm SD, unless stated otherwise. Comparisons between groups/cells were made using the two-tailed Student's *t* test with adjusted *P* values using the Holm method for multiple comparison unless stated otherwise. Statistical significance was denoted with * ($P < 0.05$) in the figures and figure legends with indicated biological replicate numbers. Statistical analysis was performed in GraphPad Prism 8.

Data Availability. RNA sequencing data have been deposited in Gene Expression Omnibus ([GSE150918](#)).

ACKNOWLEDGMENTS. We thank Dr. Steeve Boulant (Heidelberg, Germany) for providing lentiCRISPR v2-sgRNA plasmids for *IFNAR1* and *IFNLR1* KOs, Dr. Brendan Lee and the C-BASS core in BCM for lentivirus packaging plasmids, and Ms. Susan F. Venable in the Functional Genomics and Microbiome Core of the Texas Medical Center Digestive Research Core Center for performing the Luminex assays. This work was supported in part by Public Health Service grants P01AI057788, U19AI116497, U19AI144297, P30DK56338, T32DK07664, and contract HHSN2722017000381 from the National Institutes of Health; by the Cancer Prevention and Research Institute of Texas RP160283 - Baylor College of Medicine Comprehensive Cancer Training Program; by NIH P30 shared resource grant CA125123, National Institute of Environmental Health Sciences grants P30ES030285 and P42ES032725; and by the John S. Dunn Research Foundation.

1. S. M. Ahmed *et al.*, Global prevalence of norovirus in cases of gastroenteritis: A systematic review and meta-analysis. *Lancet Infect. Dis.* **14**, 725–730 (2014).
2. A. J. Hall *et al.*, Norovirus disease in the United States. *Emerg. Infect. Dis.* **19**, 1198–1205 (2013).
3. S. M. Pires *et al.*, Aetiology-specific estimates of the global and regional incidence and mortality of diarrhoeal diseases commonly transmitted through food. *PLoS One* **10**, e0142927 (2015).
4. R. L. Atmar, S. Ramani, M. K. Estes, Human noroviruses: Recent advances in a 50-year history. *Curr. Opin. Infect. Dis.* **31**, 422–432 (2018).
5. M. E. Hardy, M. K. Estes, Completion of the Norwalk virus genome sequence. *Virus Genes* **12**, 287–290 (1996).
6. M. E. Hardy, Norovirus protein structure and function. *FEMS Microbiol. Lett.* **253**, 1–8 (2005).
7. P. Chhabra *et al.*, Updated classification of norovirus genogroups and genotypes. *J. Gen. Virol.* **100**, 1393–1406 (2019).
8. R. A. Bull, J. S. Eden, W. D. Rawlinson, P. A. White, Rapid evolution of pandemic noroviruses of the GII.4 lineage. *PLoS Pathog.* **6**, e1000831 (2010).
9. M. K. Jones *et al.*, Enteric bacteria promote human and mouse norovirus infection of B cells. *Science* **346**, 755–759 (2014).
10. M. K. Jones *et al.*, Human norovirus culture in B cells. *Nat. Protoc.* **10**, 1939–1947 (2015).
11. K. Ettayebi *et al.*, Replication of human noroviruses in stem cell-derived human enteroids. *Science* **353**, 1387–1393 (2016).
12. J. Van Dycke *et al.*, A robust human norovirus replication model in zebrafish larvae. *PLoS Pathog.* **15**, e1008009 (2019).
13. D. Zhang *et al.*, Human intestinal organoids express histo-blood group antigens, bind norovirus VLPs, and support limited norovirus replication. *Sci. Rep.* **7**, 12621 (2017).
14. S. Sato *et al.*, Human norovirus propagation in human induced pluripotent stem cell-derived intestinal epithelial cells. *Cell. Mol. Gastroenterol. Hepatol.* **7**, 686–688.e5 (2019).
15. U. C. Karandikar *et al.*, Detection of human norovirus in intestinal biopsies from immunocompromised transplant patients. *J. Gen. Virol.* **97**, 2291–2300 (2016).
16. V. Costantini *et al.*, Human norovirus replication in human intestinal enteroids as model to evaluate virus inactivation. *Emerg. Infect. Dis.* **24**, 1453–1464 (2018).
17. G. Alvarado *et al.*, Human monoclonal antibodies that neutralize pandemic GII.4 noroviruses. *Gastroenterology* **155**, 1898–1907 (2018).
18. M. C. Chan *et al.*, Use of human intestinal enteroids to detect human norovirus infectivity. *Emerg. Infect. Dis.* **25**, 1730–1735 (2019).
19. M. K. Estes *et al.*, Human norovirus cultivation in nontransformed stem cell-derived human intestinal enteroid cultures: Success and challenges. *Viruses* **11**, 638 (2019).
20. K. Murakami *et al.*, Bile acids and ceramide overcome the entry restriction for GII.3 human norovirus replication in human intestinal enteroids. *Proc. Natl. Acad. Sci. U.S.A.* **117**, 1700–1710 (2020).
21. K. Haga *et al.*, Genetic manipulation of human intestinal enteroids demonstrates the necessity of a functional fucosyltransferase 2 gene for secretor-dependent human norovirus infection. *MBio* **11**, e00251-20 (2020).
22. J. W. Schoggins *et al.*, Pan-viral specificity of IFN-induced genes reveals new roles for cGAS in innate immunity. *Nature* **505**, 691–695 (2014).
23. S. Koyama, K. J. Ishii, C. Coban, S. Akira, Innate immune response to viral infection. *Cytokine* **43**, 336–341 (2008).
24. G. Subramanian *et al.*, The interferon-inducible protein TDRD7 inhibits AMP-activated protein kinase and thereby restricts autophagy-independent virus replication. *J. Biol. Chem.* **295**, 6811–6822 (2020).
25. Y. Li *et al.*, Interferon- λ attenuates rabies virus infection by inducing interferon-stimulated genes and alleviating neurological inflammation. *Viruses* **12**, 405 (2020).
26. T. Nelemans, M. Kikkert, Viral innate immune evasion and the pathogenesis of emerging RNA virus infections. *Viruses* **11**, 961 (2019).
27. A. García-Sastre, Ten strategies of interferon evasion by viruses. *Cell Host Microbe* **22**, 176–184 (2017).
28. S. López, L. Sánchez-Tacuba, J. Moreno, C. F. Arias, Rotavirus strategies against the innate antiviral system. *Annu. Rev. Virol.* **3**, 591–609 (2016).
29. M. K. Holly, J. G. Smith, Adenovirus infection of human enteroids reveals interferon sensitivity and preferential infection of goblet cells. *J. Virol.* **92**, e00250-18 (2018).
30. L. Qu *et al.*, Replication of human norovirus rRNA in mammalian cells reveals lack of interferon response. *J. Virol.* **90**, 8906–8923 (2016).
31. W. Dang *et al.*, IRF-1, RIG-I and MDA5 display potent antiviral activities against norovirus coordinately induced by different types of interferons. *Antiviral Res.* **155**, 48–59 (2018).
32. L. Lin *et al.*, Replication and transcriptional analysis of human noroviruses in human intestinal enteroids. *Am. J. Transl. Res.* **11**, 3365–3374 (2019).
33. M. Hosmillo *et al.*, Norovirus replication in human intestinal epithelial cells is restricted by the interferon-induced JAK/STAT signaling pathway and RNA polymerase II-mediated transcriptional responses. *MBio* **11**, e00215-20 (2020).
34. D. Enosi Tuipulotu, N. E. Netzler, J. H. Lun, J. M. Mackenzie, P. A. White, TLR7 agonists display potent antiviral effects against norovirus infection via innate stimulation. *Antimicrob. Agents Chemother.* **62**, e02417-17 (2018).
35. K. O. Chang, D. W. George, Interferons and ribavirin effectively inhibit Norwalk virus replication in replicon-bearing cells. *J. Virol.* **81**, 12111–12118 (2007).
36. K. Saxena *et al.*, A paradox of transcriptional and functional innate interferon responses of human intestinal enteroids to enteric virus infection. *Proc. Natl. Acad. Sci. U.S.A.* **114**, E570–E579 (2017).
37. A. Subramanian *et al.*, Gene set enrichment analysis: A knowledge-based approach for interpreting genome-wide expression profiles. *Proc. Natl. Acad. Sci. U.S.A.* **102**, 15545–15550 (2005).
38. P. Kapranov *et al.*, RNA maps reveal new RNA classes and a possible function for pervasive transcription. *Science* **316**, 1484–1488 (2007).
39. H. Kambara *et al.*, Negative regulation of the interferon response by an interferon-induced long non-coding RNA. *Nucleic Acids Res.* **42**, 10668–10680 (2014).
40. M. Barriocanal, E. Carnero, V. Segura, P. Fortes, Long non-coding RNA BST2/BISP is induced by IFN and regulates the expression of the antiviral factor tetherin. *Front. Immunol.* **5**, 655 (2015).
41. K. Pervolaraki *et al.*, Type I and type III interferons display different dependency on mitogen-activated protein kinases to mount an antiviral state in the human gut. *Front. Immunol.* **8**, 459 (2017).
42. M. S. Hakim *et al.*, Basal interferon signaling and therapeutic use of interferons in controlling rotavirus infection in human intestinal cells and organoids. *Sci. Rep.* **8**, 8341 (2018).
43. L. Li *et al.*, Porcine intestinal enteroids: A new model for studying enteric coronavirus porcine epidemic diarrhea virus infection and the host innate response. *J. Virol.* **93**, e01682-18 (2019).
44. L. Li *et al.*, IFN-lambda 3 mediates antiviral protection against porcine epidemic diarrhea virus by inducing a distinct antiviral transcript profile in porcine intestinal epithelia. *Front. Immunol.* **10**, 2394 (2019).
45. A. O. Kolawole *et al.*, Astrovirus replication in human intestinal enteroids reveals multi-cellular tropism and an intricate host innate immune landscape. *PLoS Pathog.* **15**, e1008057 (2019).
46. C. Good, A. I. Wells, C. B. Coyne, Type III interferon signaling restricts enterovirus 71 infection of goblet cells. *Sci. Adv.* **5**, eaau4255 (2019).
47. J. Huang *et al.*, Inhibition of type I and type III interferons by a secreted glycoprotein from Yaba-like disease virus. *Proc. Natl. Acad. Sci. U.S.A.* **104**, 9822–9827 (2007).
48. L. J. Reed, H. Muench, A simple method of estimating fifty percent endpoints. *Am. J. Epidemiol.* **27**, 493–497 (1938).
49. K. O. Chang, S. V. Sosnovtsev, G. Belliot, A. D. King, K. Y. Green, Stable expression of a Norwalk virus RNA replicon in a human hepatoma cell line. *Virology* **353**, 463–473 (2006).
50. S. E. Arthur, F. Sorgeloos, M. Hosmillo, I. G. Goodfellow, Epigenetic suppression of interferon lambda receptor expression leads to enhanced human norovirus replication in vitro. *MBio* **10**, e02155-19 (2019).
51. C. G. Drummond *et al.*, Enteroviruses infect human enteroids and induce antiviral signaling in a cell lineage-specific manner. *Proc. Natl. Acad. Sci. U.S.A.* **114**, 1672–1677 (2017).
52. K. Y. Green, Norovirus infection in immunocompromised hosts. *Clin. Microbiol. Infect.* **20**, 717–723 (2014).
53. M. Eslam, J. George, Targeting IFN- λ : Therapeutic implications. *Expert Opin. Ther. Targets* **20**, 1425–1432 (2016).
54. P. M. George, R. Badiger, W. Alazawi, G. R. Foster, J. A. Mitchell, Pharmacology and therapeutic potential of interferons. *Pharmacol. Ther.* **135**, 44–53 (2012).
55. G. Schwank *et al.*, Functional repair of CFTR by CRISPR/Cas9 in intestinal stem cell organoids of cystic fibrosis patients. *Cell Stem Cell* **13**, 653–658 (2013).
56. S. Ding *et al.*, STAG2 deficiency induces interferon responses via cGAS-STING pathway and restricts virus infection. *Nat. Commun.* **9**, 1485 (2018).
57. D. M. Santer *et al.*, Differential expression of interferon-lambda receptor 1 splice variants determines the magnitude of the antiviral response induced by interferon-lambda 3 in human immune cells. *PLoS Pathog.* **16**, e1008515 (2020).
58. M. Morelli, K. M. Ogden, J. T. Patton, Silencing the alarms: Innate immune antagonism by rotavirus NSP1 and VP3. *Virology* **479–480**, 75–84 (2015).
59. S. M. Karst, C. E. Wobus, M. Lay, J. Davidson, H. W. Virgin 4th, STAT1-dependent innate immunity to a Norwalk-like virus. *Science* **299**, 1575–1578 (2003).
60. C. E. Wobus *et al.*, Replication of Norovirus in cell culture reveals a tropism for dendritic cells and macrophages. *PLoS Biol.* **2**, e432 (2004).
61. M. T. Baldrige *et al.*, Expression of Ifnlr1 on intestinal epithelial cells is critical to the antiviral effects of interferon lambda against norovirus and reovirus. *J. Virol.* **91**, e02079-16 (2017).
62. S. Marionneau *et al.*, Norwalk virus binds to histo-blood group antigens present on gastroduodenal epithelial cells of secretor individuals. *Gastroenterology* **122**, 1967–1977 (2002).

63. L. Lindesmith *et al.*, Human susceptibility and resistance to Norwalk virus infection. *Nat. Med.* **9**, 548–553 (2003).
64. A. M. Hutson, R. L. Atmar, D. Y. Graham, M. K. Estes, Norwalk virus infection and disease is associated with ABO histo-blood group type. *J. Infect. Dis.* **185**, 1335–1337 (2002).
65. L. C. Lindesmith *et al.*, Virus-host interactions between nonsecretors and human norovirus. *Cell. Mol. Gastroenterol. Hepatol.* **10**, 245–267 (2020).
66. M. M. Lamers *et al.*, SARS-CoV-2 productively infects human gut enterocytes. *Science* **369**, 50–54 (2020).
67. S. Guix *et al.*, Norwalk virus RNA is infectious in mammalian cells. *J. Virol.* **81**, 12238–12248 (2007).
68. F. S. Le Guyader *et al.*, Aichi virus, norovirus, astrovirus, enterovirus, and rotavirus involved in clinical cases from a French oyster-related gastroenteritis outbreak. *J. Clin. Microbiol.* **46**, 4011–4017 (2008).
69. C. W. Law *et al.*, RNA-seq analysis is easy as 1-2-3 with limma, Glimma and edgeR. *F1000 Res.* **5**, 1408 (2016).
70. M. Martin, Cutadapt removes adapter sequences from high-throughput sequencing reads. *EMBnet. J.* **17**, 10 (2011).
71. S. Andrews, Fast QC: A quality control tool for high throughput sequence data (2010). <https://www.bioinformatics.babraham.ac.uk/projects/fastqc/>. Accessed 3 September 2020.
72. Y. Liao, G. K. Smyth, W. Shi, featureCounts: An efficient general purpose program for assigning sequence reads to genomic features. *Bioinformatics* **30**, 923–930 (2014).
73. O. Shalem *et al.*, Genome-scale CRISPR-Cas9 knockout screening in human cells. *Science* **343**, 84–87 (2014).
74. E. Eisenberg, E. Y. Levanon, Human housekeeping genes, revisited. *Trends Genet.* **29**, 569–574 (2013).